Journal of Cellular Physiology

Clusterin Enhances Motility of Normal and Cancer Prostate Cells through a PTEN and PHLPP1/AKT2 Circuit

Journal:	*Journal of Cellular Physiology*
Manuscript ID	JCP-18-0425.R1
Wiley - Manuscript type:	Original Research Article
Date Submitted by the Author:	26-Oct-2018
Complete List of Authors:	Bertacchini, Jessika; University of Modena and Reggio Emilia, Department of Biomedical, Metabolic and Neural Sciences, Section of Morphology, Signal Transduction Unit, University of Modena and Reggio Emilia, Italy Mediani, Laura; Department of Biomedical, Metabolic and Neural Sciences, Section of Morphology, University of Modena and Reggio Emilia, Largo del Pozzo 71, 41124-Italy Beretti, Francesca; Department of Surgery, Medicine, Dentistry and Morphological Sciences, University of Modena and Reggio Emilia, Modena, Italy. Guida, Marianna; University of Modena and Reggio Emilia, Department of Biomedical, Metabolic and Neural Sciences, Section of Morphology, Signal Transduction Unit, University of Modena and Reggio Emilia, Italy Ghalali, Aram ; Institute of Environment Medicine. Karolinska Institutet, Stockholm, Sweden. Brugnoli, Federica; Department of Morphology, Surgery and Experimental Medicine, Section of Anatomy and Histology, University of Ferrara, Ferrara, Italy. Bertagnolo, Valeria; Department of Morphology, Surgery and Experimental Medicine, Section of Anatomy and Histology, University of Ferrara, Ferrara, Italy. Petricoin III, Emanuel; George Mason University, Center for Applied Proteomics and Molecular Medicine Poti', Francesco; Department of Medicine and Surgery - Unit of Neurosciences, University of Parma, via Volturno 39/F, 43125 Parma, Italy. Electronic address: francesco.poti@unipr.it. Arioli, Jessica; Department of Biomedical, Metabolic and Neural Sciences, Section of Morphology, Signal Transduction Unit, University of Modena and Reggio Emilia, Largo del Pozzo 71, 41124-Italy Anselmi, Laura; Department of Biomedical, Metabolic and Neural Sciences, Section of Morphology, Signal Transduction Unit, University of Modena and Reggio Emilia, Largo del Pozzo 71, 41124-Italy Bari, Alessia; Department of Diagnostic, Clinical and Public Health Medicine, University of Modena and Reggio Emilia McCubrey, James; Brody School of Medicine, Microbiology & Immunology Martelli, Alberto; IGM-CNR, Bologna Unit Cocco, Lucio; University of Bologna, Biomedical and Neuromotor Sciences

	Capitani, Silvano; University of Ferrara, Morphology and Embryology/Section of Human Anatomy Marmiroli, Sandra; Department of Biomedical, Metabolic and Neural Sciences, Section of Morphology, Signal Transduction Unit, University of Modena and Reggio Emilia, Largo del Pozzo 71, 41124-Italy;
Key Words:	Akt2, PHLPP1, miR-190, clusterin, prostate cancer

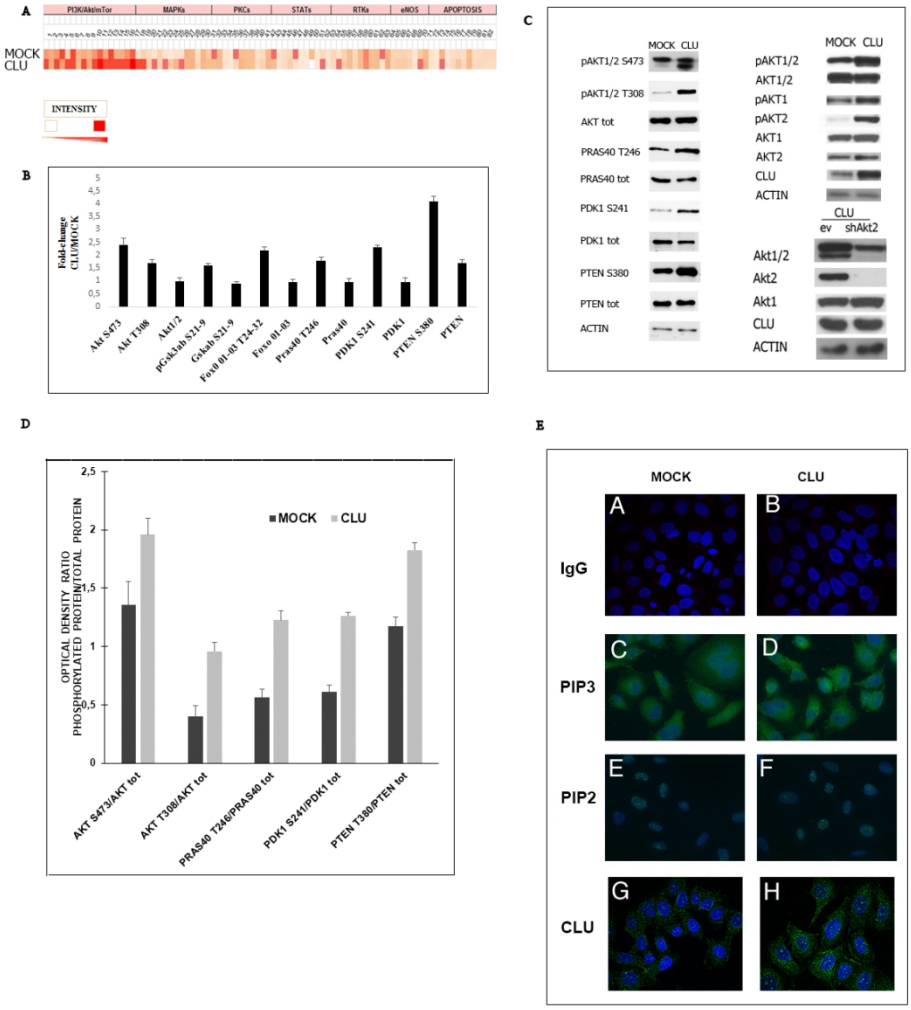

Clusterin enhances the PI3K signaling pathway at multiple levels

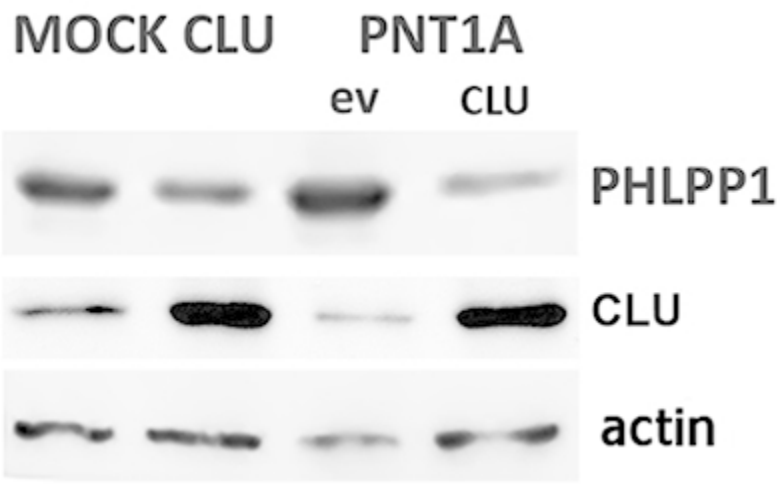

Analysis of PHLPP1 levels in CLU overexpressing cells.

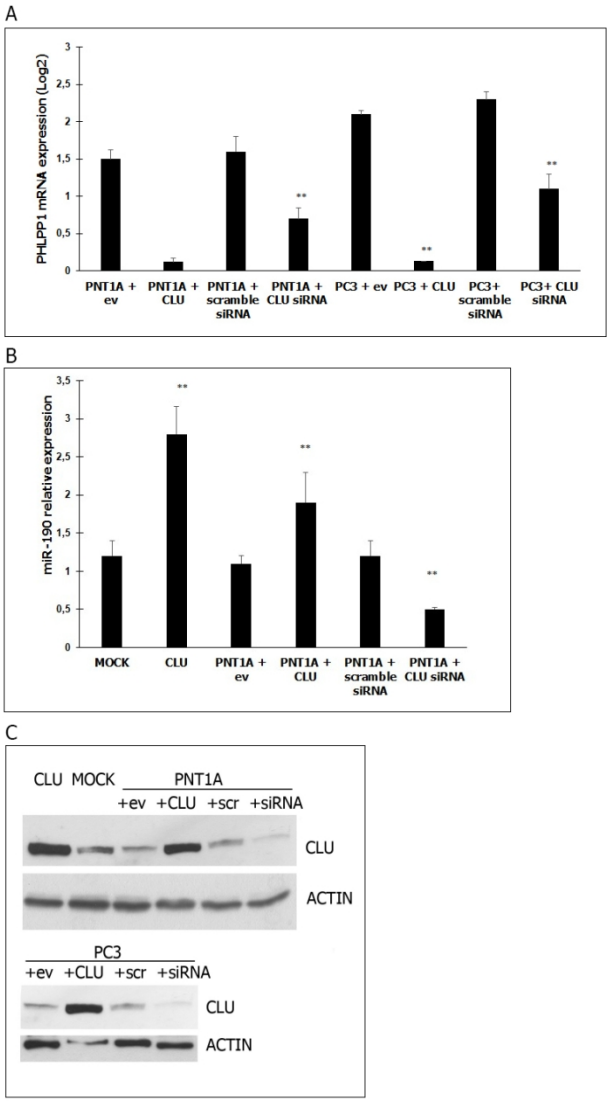

Modulation of PHLPP1 expression by CLU.

74x129mm (300 x 300 DPI)

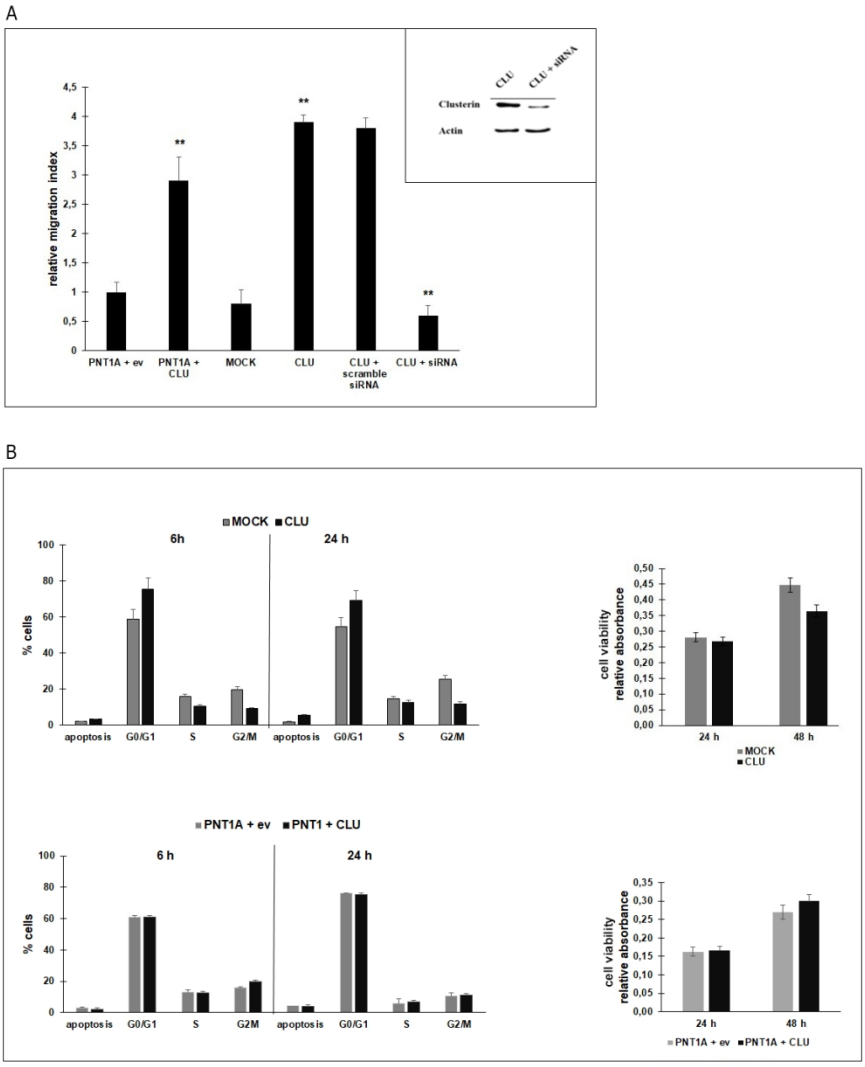

CLU stimulates migration of normal prostate cells.

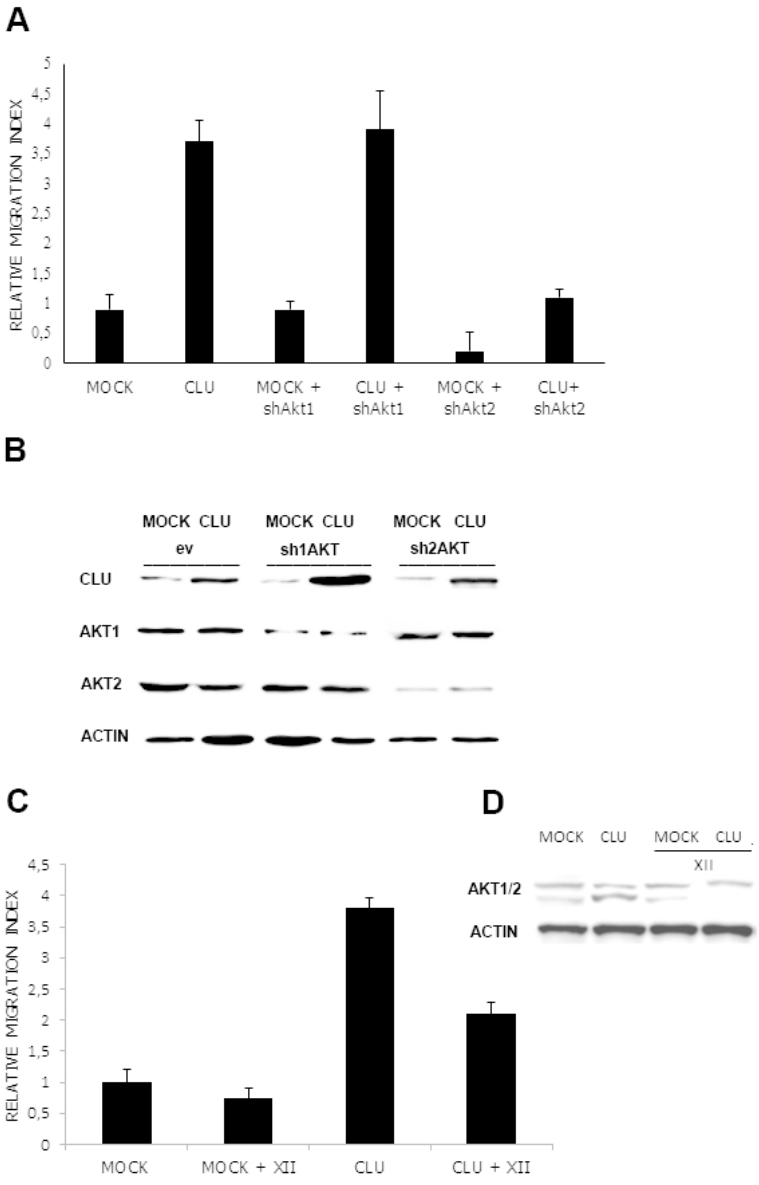

Effect of AKT isoform-silencing on CLU-stimulated cell migration.

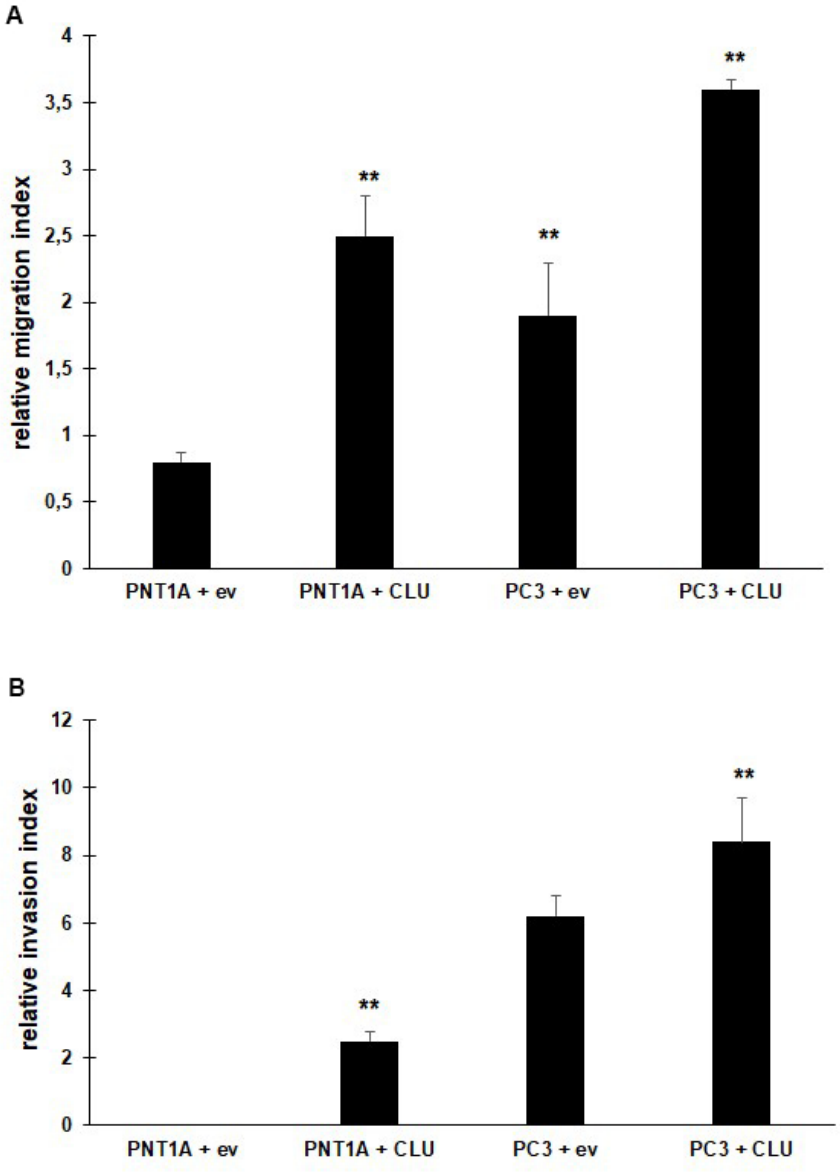

Modulation of normal and cancer cell motility by CLU.

Antibody	Dilution RPPA	Supplier
1. phospho-Akt S473	1:100	CST
2. phospho-Akt T308	1:100	CST
3. Akt1/2	1:100	CST
4. phospho-GSK3α/β S21-9	1:100	BioSource
5. GSK3α/β	1:100	CST
6. phospho-FoxO1-O3 T24-32	1:100	CST
7. FoxO1-O3	1:100	CST
8. phospho-PRAS40 T246	1:1000	BioSource
9. PRAS40	1:1000	CST
10. phospho-PDK1 S241	1:200	CST
11. PDK1	1:100	CST
12. phospho-PTEN S380	1:500	CST
13. PTEN	1:100	CST
14. phospho-P70 6SK	1:100	CST
15. phospho-CREB S133	1:100	CST
16. phospho-4EBP1 S65	1:100	CST
17. EGFR	1:100	BioSource
18. ERK	1:100	CST
19. CICasp3 (D175)	1:50	CST
20. phospho-AcetylCoA S79	1:100	CST
21. phospho-ERK T202-Y204	1:100	CST
22. phospho-FKHR S256	1:100	CST
23. phospho-FKHRL1 S253	1:100	CST
24. phospho-IRS1 S612	1:200	CST
25. phospho-PDGFRB Y716	1:100	CST
26. phospho-STAT1 Y701	1:100	CST
27. phospho-STAT3 S727	1:50	CST
28. phospho-STAT3 Y705	1:50	CST
29. phospho-ABL T735	1:50	CST
30. phospho-ABL Y245	1:100	CST
31. phospho-AMPKA S485	1:100	CST
32. phospho-AMPKB S108	1:100	CST
33. phospho-ARRESTINIB1 S412	1:100	CST
34. phospho-ASK1 S612	1:50	CST
35. phospho-BAD S112	1:200	CST
36. phospho-BAD S136	1:200	CST
37. phospho-Bcl2 S70	1:100	CST
38. phospho-Bcl2 T56	1:100	CST
39. ClCasp9 D330	1:50	CST
40. phospho-β-Catenin S33-35-T41	1:100	CST
41. phospho-Cofilin S3	1:100	CST
42. phospho-EGFR Y992	1:50	CST
43. phospho-EGFR Y1045	1:100	CST
44. phospho-EGFR Y1068	1:100	CST
45. phospho-EGFR Y1148	1:100	CST
46. phospho-EGFR Y1173	1:100	CST
47. phospho-EIF4E S209	1:100	CST
48. phospho-EIF4G S1108	1:100	CST
49. phospho-eNOS S113	1:100	CST
50. phospho-eNOS S1177	1:100	CST
51. eNOS S116	1:100	Upstate
52. phospho-ERB2HER2 Y1248	1:100	Upstate
53. phospho-ERB3HER3 Y1289	1:100	Upstate
54. phospho-ETK Y40	1:100	CST
55. phospho-FADD S194	1:50	CST
56. phospho-FAK Y576-577	1:100	BD
57. phospho-HISTONEH3 S10	1:100	Upstate
58. phospho-LKB1 S334	1:100	CST
59. phospho-LKB1 S428	1:100	CST
60. phospho-MARCKS S152-156	1:100	CST

61. phospho-MEK1 S217-221	1:100	CST
62. phospho-pan-PKC	1:100	CST
63. phospho-P38	1:100	CST
64. phospho-P90RSK	1:100	CST
65. phospho-PKA T197	1:100	CST
66. phospho-PKCα S257	1:100	CST
67. phospho-PKCαβ T638-641	1:100	CST
68. phospho-NFκB S536	1:100	CST
69. phospho-PKCδ T505	1:100	CST
70. phospho-PKCθ T538	1:100	CST
71. phospho-PKCζλ T410-403	1:100	CST
72. phospho-A RAF S299	1:100	CST
73. phospho-B RAF S445	1:100	CST
74. phospho-C RAF S338	1:200	CST
75. phospho-RAS GRF1 S916	1:100	CST
76. phospho-RSK3 T356-360	1:100	CST
77. phospho-S6rb S235-S36	1:200	CST
78. phospho-SMAD2 S465-467	1:250	CST
79. phospho-STAT5 Y694	1:50	CST
80. phospho-IKBα S32-36	1:50	BD
81. eNOS	1:100	CST
82. NFκB	1:50	CST
Antibody	**Dilution Western blot**	**Supplier**
83. phospho-GSK3α/β S21-9	1:1000	CST
84. GSK3α/β	1:1000	BioSource
85. phospho-FoxO1-O3 T24-32	1:1000	CST
86. FoxO1-O3	1:1000	CST
87. phospho-PRAS40 T246	1:1000	CST
88. PRAS40	1:1000	BioSource
89. phospho-PDK1 S241	1:2000	CST
90. PDK1	1:1000	CST
91. phospho-PTEN S380	1:500	CST
92. PTEN	1:1000	CST
93. PHLPP1	1:1000	Bethyl Laboratories Inc
94. pAkt S473/S474	1:1000	CST
95. HA	1:1000	Sigma-Aldrich
96. Clusterin	1:500	Santa Cruz
97. Actin	1:1000	Sigma-Aldrich
98. Akt1/2	1:1000	CST
99. Akt1	1:1000	CST
100. Akt2	1:1000	CST

Table 1S. Antibody list. The table provides a complete list of the antibodies used in the work, of their working dilution and of suppliers.

Clusterin Enhances AKT2-mediated Motility of Normal and Cancer Prostate Cells through a PTEN and PHLPP1 Circuit.

Jessika Bertacchini[1#], Laura Mediani[1], Francesca Beretti[2], Marianna Guida[1], Aram Ghalali[3], Federica Brugnoli[4], Valeria Bertagnolo[4], Emanuel Petricoin[5], Francesco Poti[6], Jessica Arioli[1], Laura Anselmi[1], Alessia Bari[7], James McCubrey[8], Alberto M. Martelli[9], Lucio Cocco[9], Silvano Capitani[4], Sandra Marmiroli[1#].

[1]Department of Biomedical, Metabolic and Neural Sciences, Section of Morphology, Signal Transduction Unit, University of Modena and Reggio Emilia, Largo del Pozzo 71, 41124-Italy; [2]Department of Medicine, Surgery, Dentistry and Morphology, University of Modena and Reggio Emilia, Largo del Pozzo 71, 41124-Italy; [3]Institute of Environment Medicine, Karolinska Institutet, Stockholm, 21017177-Sweden; [4]Department of Morphology, Surgery and Experimental Medicine, Section of Anatomy and Histology and LTTA Center, via Fossato di Mortara 70, University of Ferrara, 44121-Italy; [5]Center for Applied Proteomics & Molecular Medicine, GMU, Fairfax, VA 22030, USA; [6]Department of Medicine and Surgery-Unit of Neurosciences, University of Parma, via Volturno 39/F, 43125-Italy; [7]Program of Innovative Therapy in Oncology and Hematology, Department of Diagnostic, Clinical Medicine and Public Health, University of Modena and Reggio Emilia, Largo del Pozzo 71, 41124-Italy; [8]Department of Microbiology and Immunology, Brody School of Medicine at East Carolina University, Greenville, NC 27858, USA; [9]Department of Biomedical and NeuroMotor Sciences, University of Bologna, via Irnerio 48, 40136-Italy.

#Correspondence to:

Sandra Marmiroli Largo del Pozzo 71, 41124 Modena-Italy. sandra.marmiroli@unimore.it; tel 00390594224833; fax 00390594224861

Jessika Bertacchini Largo del Pozzo 71, 41124 Modena-Italy. Jessika.bertacchini@unimore.it; tel 00390594224842; fax 00390594224861

Running title: Clusterin-regulated miR-190/PHLPP1/AKT2/PTEN circuit

ABSTRACT

Clusterin (CLU) is a chaperone-like protein with multiple functions. sCLU is frequently up-regulated in prostate tumor cells following chemo or radio therapy and following surgical or pharmacological castration. Moreover, CLU has been documented to modulate AKT activity. Here we investigated how CLU overexpression influences PI3K/AKT signaling in human normal and cancer epithelial prostate cells. Human prostate cells stably transfected with CLU were broadly profiled by reverse phase protein array (RPPA), with particular emphasis on the PI3K/AKT pathway. The effect of CLU overexpression on normal and cancer cell motility was also tested. Our results clearly indicate that CLU overexpression enhances phosphorylation of AKT restricted to isoform 2. Mechanistically, this can be explained by the finding that the phosphatase PHLPP1, known to dephosphorylate AKT2 at S474, is markedly downregulated by CLU, whereas miR-190, a negative regulator of PHLPP1, is up-regulated. Moreover, we found that PTEN was heavily phosphorylated at the inhibitory site S380, contributing to the hyperactivation of AKT signaling. By keeping AKT2 phosphorylation high, CLU dramatically enhances the migratory behavior of prostate epithelial cell lines with different migratory and invasive phenotype, namely PNT1A and PC3 cells. All together, our results unravel for the first time a circuit by which CLU can switch a low migration phenotype towards a high migration phenotype, through miR-190-dependent down-modulation of PHLPP1 expression and, in turn, stabilization of AKT2 phosphorylation.

INTRODUCTION

The many functions of the ubiquitously expressed protein clusterin (CLU) are mirrored by the multiplicity of its names (Apoliprotein J, Testosterone-repressed prostate message 2, Sulfate glyprotein-2 among others). Under physiological condition, the predominant translation product of the human gene is a 80 kDa heterodimeric, disulfide-linked and highly glycosylated secretory protein, sCLU, mainly characterized by chaperoning function as well as cytoprotective activity (1-9). This cytoprotective chaperoning role is particularly evident upon stress where sCLU increases the solubility of denatured proteins and mediates the uptake and degradation of a broad spectrum of hydrophobic denatured aggregated molecules (10,11). Moreover, sCLU associates to, and stabilizes, the Ku70-Bax complex in the cytoplasm (12,13) and is therefore believed to play an important role in survival and resistance to chemotherapeutic drugs (14,15). However, the elucidation of CLU broad range of functions has been partly hampered by the finding that, under cell stress or damage a number of forms can be produced from the evolutionary conserved *CLU* gene either through alternative splicing/non canonical translation/initiation start sites or eluding the glycosylation steps necessary to secretion (7-8). These intracellular forms display different intracellular localization and, in some case, almost opposite biological functions (16-19).

Interestingly, CLU has been shown to affect the phosphatidylinositol 3'-kinase (PI3K)-AKT pathway (20-22). This pathway is a central hub of oncogenic signaling and has been linked to tumorigenesis in a wide variety of tumor types (23,24). In normal cells, stimulation of growth factor receptors activates acute production of phosphatidylinositol-3,4,5-triphosphate (PIP_3) by PI3K, thus triggering dual AKT phosphorylation: at T308, by PDK1, and at S473, by mTORC2. Fully active AKT, in turn, enhances cell proliferation and survival (25). Eventually, dephosphorylation of PIP_3 by the lipid phosphatase PTEN and/or dephosphorylation of AKT S473 by PHLPP1/2 protein phosphatases turn off AKT signaling (26-27). Activation of PI3K/AKT signaling has been

widely implicated in prostate cancer progression (23, 27-29). Molecular alterations such as mutations, chromosomal aberrations and altered expression of key pathway components have been reported in 42% of primary and 100% of metastatic prostate cancers (27, 30-31). The majority of the above abnormalities include decreased expression of PTEN and/or of PHLPPs, therefore leading to constitutively active AKT signaling. Interestingly, PHLPP1 mRNA is downregulated in high-grade prostate cancer, suggesting that PHLPP1 loss contributes with other genetic aberration to promote prostate cancer progress. Moreover, a study performed with AKT isoform-silencing showed that, opposite to other models such as breast cancer cells, AKT1 and AKT2 cooperate to enhance migration and invasion of PC3 cells through up-regulation of β1-integrin (32). On the other hand, AKT1 and AKT2 were described to play non-redundant functions in PC3 cells migration, possibly through distinct subcellular localization. Furthermore, it has been suggested that AKT isoform-specific contribution might differ during prostate cancer progression, from androgen-sensitive to hormone-resistant stage (33). Therefore, mechanistically the peculiar roles of AKT isoforms in prostate cancer cell migration and invasion, if any, have not been conclusively settled. Here, we unravel a yet-undescribed regulatory system driven by sCLU, that modulates PHLPP1 level, leading to constitutive activation of AKT2 and enhanced migration and invasion both of normal and cancer prostate cells.

MATERIALS AND METHODS

Cell Cultures and Inhibitors

Human prostate carcinoma PC3 cell line was from DSMZ (Braunschweig, Germany). Normal prostate epithelial PNT1A cells stably transfected with empty vector pIRES-hyg1 or pIRES-CLU were a kind gift from the laboratory of Dr. Saverio Bettuzzi (University of Parma, Italy) (34), and will be thereafter referred to as CLU and MOCK cells, respectively. PNT1A and PC3 cells were grown in RPMI 1640, Ham's F12 and DMEM, supplemented with 1% L-Glutamine, 10% heat-inactivated FBS (Euroclone,

Italy) and antibiotics (Sigma-Aldrich), at 37°C in a humidified atmosphere with 5% CO_2. Where indicated, the AKT2-selective inhibitor XII (Merck Millipore, Italy) was used at 0.5 μM.

MTT assay was performed in 96 well plates. Ten thousand cells/well were seeded and cells were cultured for 24 and 48 hours. MTT (Sigma-Aldrich, St. Louis, USA) was dissolved in PBS at 5 mg/mL and 20 μL of MTT solution was added to each well followed by 3 hours incubation at 37°C, 5% CO_2. Then, plates were read out by an ELISA reader (LifeTech) at 590 nm.

Cell Proliferation was monitored by Propidium Iodide (PI) staining. After harvesting, the cells were washed twice with PBS and re-suspended in 100 μl binding buffer (10 mM HEPES/NaOH, of pH 7.4, 140 mM NaCl, 2.5 mM $CaCl_2$ and 50 μg/ml PI). The samples were incubated for 10 min in the dark at 4°C and then analyzed by flow cytometry.

Transfections

For transient CLU overexpression, cells were transfected with polyethylenimine (PEI) in a 3:1 ratio of PEI (μg): total DNA (μg). Control cells were transfected with empty vector. CLU silencing was performed with specific siRNA, transfected for 72 hours with siRNA transfection reagent as described in the supplier's instruction manual. For negative control, cells were transfected with 100 nM scramble siRNA (all from Santa Cruz Biotechnology, Santa Cruz, CA). Where indicated, AKT1 and AKT2 were silenced with a set of AKT1 or AKT2 target shRNAs, kindly provided by the laboratory of Alex Toker (Beth Israel Deaconess Center, Boston, U.S.A). shAKT1 and shAKT2 were transduced in cells for 72 hours by lentiviral supernatant obtained in packaging hosts HEK293 cells as described (35). Infected cells were selected with 5 μg/ml of Puromycin for 48 hours.

Immunoblotting and Immunofluorescence

Cell lysis was performed on ice for 20 minutes in a lysis buffer suitable for both RPPA and immunoblotting, as described previously (36). Briefly, for immunoblotting, lysates were sonicated three times for 10 seconds on ice, then centrifuged at 10,000 g for 15 min at 4°C, and denatured at 100°C for

5 minutes in SDS-loading buffer, run on a 7%SDS-PAGE, then transferred to an Immobilon-P PVDF membrane (Merck Millipore, Italy) and incubated overnight at 4°C with primary antibodies (37). A list of antibodies is provided in Table 1S. For immunofluorescence, anti-PIP3 and anti-PIP2 antibodies (Echelon Biosciences, Salt Lake City, UT) were used at 1:50 dilution. Cells were analyzed using a Nikon Eclipse TE2000 inverted microscope, and fluorescent images were captured with a Hamamatsu camera (Hamamatsu City, Japan), as described previously (38-39).

RPPA

For RPPA, protein lysates were diluted to a final concentration of 0.5 mg/ml, then 30 µl were loaded on a 383-well plate and subjected to immunostaining with a panel of 82 commercially available, validated antibodies directed against specific phosphorylated or cleaved proteins, all from Cell Signaling Technology (Table 1S), as described (36, 40-41).

RNA purification and Real Time quantitative PCR

Total RNA was extracted with the RNeasy Mini Kit (Qiagen, Valencia, CA) and reverse-transcribed with the High capacity cDNA Reverse Transcription kit (Applied Biosystem, Foster City, CA) according to manufacturer's instructions. Quantification of miR-190 was performed with a miRCRY LNA Universal RT miR cDNA synthesis kit, SYBR Green master mix, Universal RT and LNA PCR primer. Primer sequences were the following: PHLPP1, Forward: 5'-TGCTCACTCCAACTGCATCGAG-3′ Reverse: 5′-GGTTTCCAGTCAGGTCTAGCTC-3′. miR-190, Forward: 5'-TGATATGTTTGATATATTAGG-3′ Reverse: 5′-GAACATGTCTGCGTATCTC-3′. GADPH, Forward: 5′-CGAGATCCCTCCAAAATCAA-3′ Reverse: 5′-TTCACACCCATGACGAACAT-3′. Relative gene expression quantification was based on the comparative threshold cycle method ($2^{-\Delta\Delta Ct}$). Raw data were normalized to the included housekeeping gene (GAPDH, glyceraldehyde 3-phosphate dehydrogenase).

Cell Migration and Invasion Assay

Migration experiments were performed both by transwell migration assay and by XCELLigence RTCA System. For transwell migration experiments, 10^5 cells were resuspended in 200 µl of RPMI + BSA 3% and added to the upper chamber of a two-chamber device separated by the porous membrane (polycarbonate membrane inserts 8-µM pore size; Corning). The lower chambers were filled with 600 µl of NIH-3T3 cells medium or with conditioned medium from CLU cells or with recombinant CLU. Cells were incubated at 37°C for 48 hours to allow cell migration through the membrane. Migratory cells were stained with HEMA 3 STAIN kit (Thermo Scientific) and counted under a Nikon Eclipse TE2000 inverted microscope. Migration and invasion experiments with the xCELLigence RTCA System (Roche Applied Science) were performed following manufacturer instructions, as described previously (42, 43). Briefly, 4×10^4 cells/well were seeded onto the top chambers of CIM-16 plates while the bottom chambers were filled with NIH-3T3 cells medium or with CLU-conditioned medium. The signal detection was programmed every 15 min for a total of 48 hours. Impedance values were expressed as relative arbitrary units.

Statistical analysis.

Data were expressed as mean ± standard deviation. Differences were tested by Student's t-test. The values $P < 0.05$ were considered statistically significant. Statistical analysis was done using the PRISM GraphPad statistical software. For RPPA, to detect differences between total protein expression and phosphorylated protein expression, a paired t-test was performed. We set 1.2-fold as the cutoff magnitude to qualify changes in specific proteins as significant.

RESULTS

CLU modulates the PI3K pathway

MOCK and CLU cells were analyzed by RPPA to compare 82 native and phosphorylated proteins operating in key signaling pathways. Several endpoints were differentially expressed or phosphorylated (Fig. 1A and Fig. 1S). In particular, CLU cells showed a marked phosphorylation of proteins involved in the PI3K/AKT/mTOR cascade, such as PDK1, PTEN, as well as AKT itself and its direct substrates PRAS40 and Foxo (Fig. 1B). This observation was confirmed by Western blotting (Fig. 1C). Although modulation of AKT activity by CLU had been shown previously (20-22), no molecular mechanism has been defined yet. We noticed that AKT phosphorylated at S473 migrated as a doublet (Fig 1C). Remarkably, while phosphorylation of the upper band was very similar in the two cell subtypes, the lower band was heavily phosphorylated in CLU cells but almost undetectable in MOCK cells. The antibody used detects AKT1, AKT2 and AKT3 phosphorylation at S473, S474 and S472, respectively, suggesting that the bands could correspond to different isoforms. However, in these cells AKT3 is almost undetectable (not shown). By means of single isoform silencing the lower band proved to be AKT2, suggesting that CLU exerts an isoform-restricted control over AKT phosphorylation (Fig. 1C, lower right panel). This result, intriguing in itself, was even more so because by the same analysis we found that the expression levels of the lipid phosphatase PTEN was almost doubled in CLU compared to MOCK cells. As PTEN dephosphorylates PIP3 (44) and is therefore a well-known negative regulator of AKT (45-47), this would suggest a decrease, rather than an increase, of AKT activity should occur. Nevertheless, along with increased PTEN expression, also PTEN phosphorylation at S380 was altered, being dramatically higher in CLU cells (Fig. 1B, C). Thus, since S380 phosphorylation is known to inhibit PTEN phosphatase activity, while stabilizing the protein against degradation (48, 49), we concluded that the high level of pS380-PTEN in CLU cells actually contributes to AKT hyperactivation. To confirm this, we compared the content of PIP3 in MOCK and CLU cells by immunofluorescence. In good agreement

with the above-mentioned results, the staining intensity of PIP3 was significantly higher in CLU cells with respect to the parental MOCK cells (Fig. 1E). In contrast, PIP2 levels were similar, suggesting that the increased PIP3 level results more from PTEN down-regulation than from PI3K activation (Fig. 1E). Although high PIP3 levels can explain the sustained PDK1 S241 and AKT T308 phosphorylation, since PI3K and PTEN activity were not measured directly, we cannot rule out that PIP3 derives from PI3K activity rather than from PTEN inactivation. To assess whether the T308 phosphatase PP2A may also contributes to this mechanism, MOCK and CLU cells were incubated for 60 minutes with okadaic acid, a well known PP2A inhibitor, then the level of phospho-T308 in the two cell types was compared. In cells treated with okadaic acid and probed with anti-pT308 we observed a strong drop of the signal. However, it is also clear that the degree of inhibition of PP2A is the same in MOCK and CLU. Although not conclusive, this result suggests that PP2A activity is similar in both cell lines (Figure 2S).

All together, these findings could account for the 2.5-fold increase in total AKT phosphorylation detected by RPPA in CLU cells, but did not explain the dramatic differential phosphorylation of AKT2-S474 in CLU cells. We therefore decided to monitor the amount of the protein phosphatase specific to AKT2-S474, namely PHLPP1. We observed that PHLPP1 was markedly downregulated in CLU compared to MOCK cells (Fig. 2), a condition which, by itself, could explain AKT2 hyperactivity. PHLPP1 down-modulation was clearly detectable not only in cells stably expressing CLU, but also in transiently transfected PNT1A cells, though to a lesser extent (Fig. 2). These results prompted us to investigate deeper the interplay between AKT2, PHLPP1 and CLU.

CLU enhances miR-190 which, in turn, down modulates PHLPP1

From RPPA analysis, it was evident that both the phosphorylation of GSK3 at its activatory residues and that of its main substrate β-catenin, at the GSK-3 site S33/S37/T41, was more than doubled in CLU cells (Fig 2S). Interestingly, Gao and coworkers demonstrated that PHLPP1 is a proteolytic target of the E3

ligase β-TrCP and undergoes proteasomal degradation upon sequential phosphorylation by CK1 and GSK3 (50). This suggested that CLU might promote GSK3-mediated PHLPP1 degradation. Moreover, we analyzed also the effect of CLU overexpression on PHLPP1 expression. Interestingly, we found that PHLPP1 mRNA was dramatically downregulated (>10 fold) in PNT1A cells transfected with CLU, compared to empty vector-transfected controls (Fig. 3A, left). Conversely, silencing of endogenous CLU by specific siRNA triggered a 6- to 8-fold increase in PHLPP1 mRNA, clearly indicating that CLU indeed modulates its transcription. As PNT1A are normal prostatic epithelial cells, we wondered whether CLU might display the same effects also in prostate cancer cells, such as the highly tumorigenic PC3 cell line. We found that the expression of PHLPP1 was unquestionably up-regulated by CLU silencing (>20 fold) and down-modulated by overexpression, with a trend similar to that observed in PNT1A cells although to a greater extent (Fig. 3A right). Recently, a number of miRs have been shown to control the expression of PHLPPs (51). In particular, miR-190 and miR-214 have been shown by us and others to regulate PHLPPs expression in prostate epithelial cells (52). Thus, we asked whether CLU might tune PHLPP1 levels through such molecules. Expression of both miR-190 and miR-214 was analyzed by RT-PCR. While the level of miR-214 was not affected (not shown), that of miR-190 was significantly higher in CLU compared to MOCK cells, and a similar increase was observed upon forced expression of CLU, particularly in PC3 cells (39-fold increase) (Fig. 3B). Thus, we conclude that CLU exerts a complex control of PHLPP1 phosphatase regulation mediated by an epigenetic mechanism involving increased expression of miR-190, which eventually leads to constitutive phosphorylation of AKT2.

CLU facilitates cell migration and invasion through a PHLPP1-AKT2 circuit.

Overexpression of CLU has been reported to enhance the metastatic behavior of human laryngeal squamous carcinoma cells (53), as well as renal (54, 55), breast (56) and hepatocellular carcinoma (57). Conversely, CLU was demonstrated to inhibit prostate cancer cell migration by association to α-actinin

and disassembling of the actin cytoskeleton (6, 58). Our results clearly indicated that CLU stable clone cells exhibited, over a 24-hour time frame, a migration index more than three-fold higher than their MOCK counterpart. On the contrary, silencing of clusterin by specific siRNA strongly inhibited migration of CLU cells (Fig. 4A). Therefore, we analyzed the effects of CLU transient overexpression on migration of PNT1A cells, which are not expected to display a high mobility phenotype. Remarkably, transient transfection of PNT1A cells for 48 hours was sufficient to boost their migration almost to the levels of CLU cells (Fig. 4A). As the transwell assay used to evaluate migration does not detects alterations of cell proliferation or cell viability, the possibility that such effects might be evoked by clusterin during the 48 hours time frame were ruled out by means of analysis of the cell cycle through PI staining and flow cytometry as well as of the viability by MTT assay (Fig. 4B).

Next, we explored the effect of AKT silencing on migration of MOCK versus CLU cells. We found that while AKT1 silencing affected migration of neither MOCK nor CLU cells, silencing of AKT2 prevented migration of both cell types (Fig. 5A). Treatment with the AKT2-selective pharmacological inhibitor AKT Inhibitor XII (59, 60) at a dose as low as 500 nM, gave similar results (Fig. 5C). All together, these findings indicate that CLU likely controls prostate epithelial cell migration predominantly through down-regulation of PHLPP1 and activation of AKT2.

Next, we investigated how CLU might affect movement of prostate cancer cells with an invasive phenotype. Thus, the migration capability of PNT1A cells was compared to that PC3 cells, which display increased invasiveness, upon transfection with either empty vector or with CLU. As expected, PC3 cells displayed a higher basal migration index than PNT1A, which was nevertheless dramatically increased by overexpression of CLU in both cell types (Fig. 6A). What's more important, we further evaluated the effects of CLU expression in cells grown in a 3D matrix. The results are clear and show that CLU overepression significantly stimulated cell invasion through Matrigel (Fig. 6B). These results are in complete agreement with the observation that expression of CLU increases, whereas its silencing

decreases, PHLPP1 expression in both PNT1A and PC3 cells, while inversely affects MiR-190, and allow altogether to conclude that CLU exerts a pro-migration and pro-invasion effect on healthy epithelial prostate cells through a miR-190/PHLPP1/AKT 2 circuit.

DISCUSSION

CLU is a small heat-shock-like protein overexpressed in many solid tumors, with multiple functions but largely elusive molecular mechanisms. Work from independent laboratories has suggested that it can modulate the PI3K/AKT pathway, although in a cell-type and context dependent manner. In particular, CLU has been shown to block PI3K activity through association with IGF-1 and inhibition of IGF-1R during serum deprivation (20), to mediate IGF-1 induced activation of PI3K signaling in non-small cell lung cancer (22) or to activate AKT and promote survival of prostate cancer cells (21). On the other hand, AKT has been shown to upregulate sCLU which, in turn, would mediate docetaxel resistance in prostate cancer cells (61). By a wide analysis of the phosphoproteome of normal prostate PNT1A cells overexpressing CLU, the first part of our study shows that CLU impinges on the PI3K/AKT cascade at multiple levels and, by doing so, hyperactivates AKT. The enhanced phosphorylation of AKT at T308 could be explained by our finding that in CLU cells the specific PIP3 phosphatase PTEN (44) is highly phosphorylated at the inhibitory site T380 (48). However, we unambiguously demonstrate for the first time that CLU also evokes a dramatic differential phosphorylation of AKT2. Although the parallel inactivation of PTEN can undeniably contribute to AKT2 activation, it cannot account for the observed isoform selectivity. Taking advantage of the notion that the phosphatases which dephosphorylate AKT at S473 display isoform-specific activity (26, 27), we disclose here that the AKT2-specific phosphatase, PHLPP1, is strongly down-regulated in CLU cells. PHLPP1 has been reported to undergo proteasome-dependent degradation following phosphorylation by GSK3 and CK1 in colon cancer cells (50). While on the one hand our results suggest that CLU overexpression might in part promote such mechanism also in normal prostate cells, on the other hand we have clearly demonstrated that CLU mainly acts by

preventing mRNA translation of PHLPP1. Importantly, since it has been recently demonstrated that PHLPP expression can be modulated through specific miRs (52), and in particular in prostate cancer cells by the upregulation of miR-190 and miR-214, we investigated whether CLU alters the expression of these molecules. Although we did not observe any change in miR-214 level, we were able to show that the intracellular content of miR-190 in cells either transfected with or exposed to CLU is indeed affected to a very large extent (up to a 39-fold increase in PC3 cells). An opposite result was obtained by CLU silencing. In light of the effects of CLU on PHLPP1 expression and the resulting peculiar phosphorylation pattern of AKT isoforms, we assessed whether CLU might affect cell motility. Pioneering work by Bettuzzi and coworkers suggested that CLU counteracts cell migration and invasion (34). Conversely, more recent works from different laboratories indicate that it enhances cell migration in several cell models (56, 62). Although there is some evidence that in macrophages CLU promotes chemotactic migration through up-regulation of matrix metalloproteinase-9 and NF-kB activation downstream of AKT and Erk1/2 (63, 64), hitherto its molecular mechanisms in prostate cells have remained elusive. We show that overexpression of CLU triggers migration both in normal and in cancer prostate cells, and is sufficient to increase the migration index of normal PNT1A cells to the same level of the highly metastatic PC3 prostate cancer cells. Conversely, CLU silencing prevents migration in both cell types. In particular, based on the effects of specific silencing of either AKT1 or AKT2, we further demonstrate that CLU drives cell migration through AKT2. Inhibition of AKT2 activity by the isoform-specific allosteric inhibitor AKTi XII supported this conclusion. CLU-induced decrease in PHLPP1 expression is in complete agreement with this function of AKT2. Moreover, we demonstrate that CLU overexpression is sufficient to boost PC3 cell invasion through a 3D Matrigel, whereas CLU silencing completely abrogates it.

Thus, all together our results clearly demonstrate for the first time that CLU pro-migration activity is controlled by the PHLPP/AKT axis, as CLU can switch the low migration and invasion phenotype of

normal prostate cells towards the high migration phenotype typical of cancer PC3 cells through the modulation of the expression of PHLPP1 and, in turn, the activity of AKT2.

Acknowledgements

The authors thank the laboratory of Dr. Bettuzzi for providing MOCK and CLU clones, as well as CLU expression vector. This work was supported by grants from Fondazione Cassa Risparmio Vignola to SM.

Conflict of Interest

The authors declare no conflict of interest.

References

1. Choi-Miura NH, Takahashi Y, Nakano Y, Tobe T, Tomita M (1992) Identification of the disulfide bonds in human plasma protein SP-40 (apolipoprotein-J). *J Biochem* **112**: 557-61
2. Rosenberg ME and Silkensen J (1995) Clusterin: physiologic and pathophysiologic considerations. *Int J Biochem Cell Biol* **27**: 633-45
3. Leskov KS, Klokov DY, Li J, Kinsella TJ, Boothman DA (2003) Synthesis and functional analyses of nuclear clusterin, a cell death protein. *J Biol Chem* **278**: 11590-600
4. Shannan B, Seifert M, Leskov K, Willis J, Boothman D, Tilgen W, Reichrath J (2006) Challenge and promise: roles for clusterin in pathogenesis, progression and therapy of cancer. *Cell Death Diff* **13**: 12-9
5. Pucci S, Mazzarelli P, Nucci C, Ricci F, Spagnoli LG (2009) CLU "in and out": looking for a link. *Adv Cancer Res* **105**: 93-113
6. Rizzi F and Bettuzzi S (2010) The clusterin paradigm in prostate and breast carcinogenesis. *Endocr Relat Cancer* **17**: R1-17

7. Prochnow H, Gollan R, Rohne P, Hassemer M, Koch-Brandt C, Baiersdörfer M (2013) Non-secreted clusterin isoforms are translated in rare amounts from distinct human mRNA variants and do not affect Bax-mediated apoptosis or the NF-κB signaling pathway. *PLoS One* **8**:e75303
8. Bonacini M, Coletta M, Ramazzina I, Naponelli V, Modernelli A, Davalli P, Bettuzzi S, Rizzi F (2015) Distinct promoters, subjected to epigenetic regulation, drive the expression of two clusterin mRNAs in prostate cancer cells. *Biochim Biophys Acta* **1849**:44-54
9. Kim N, Choi WS (2011) Proapoptotic role of nuclear clusterin in brain. *Anatomy & Cell Biology* **44**: 169-175
10. Viard I, Wehrli P, Jornot L, Bullani R, Vechietti JL, Schifferli JA, Tschopp J, French LE (1999) Clusterin gene expression mediates resistance to apoptotic cell death induced by heat shock and oxidative stress. *J Invest Dermatol* **112**: 290-6
11. Poon S, Treweek TM, Wilson MR, Easterbrook-Smith SB, Carver JA (2002) Clusterin is an extracellular chaperone that specifically interacts with slowly aggregating proteins on their off-folding pathway. *FEBS Lett* **513**: 259-66
12. Djeu JY and Wei S (2009) Clusterin and chemoresistance. *Adv Cancer Res* **105**: 77-92
13. Pucci S, Polidoro C, Joubert A, Mastrangeli F, Tolu B, Benassi M, Fiaschetti V, Greco L, Miceli R, Floris R, Novelli G, Orlandi A, Santoni R (2017) Ku70, Ku80, and sClusterin: A Cluster of Predicting Factors for Response to Neoadjuvant Chemoradiation Therapy in Patients With Locally Advanced Rectal Cancer. *Int J Radiat Oncol Biol Phys* **97**: 381-388
14. Koltai T (2014) Clusterin: a key player in cancer chemoresistance and its inhibition. *Onco Targets Ther* **7**: 447-56
15. Zhou J, Chen X, Gilvary DL, Tejera MM, Eksioglu EA, Wei S, Djeu JY (2015) HMGB1 induction of clusterin creates a chemoresistant niche in human prostate tumor cells. *Sci Rep* **5**:15085
16. Al Nakouzi N, Wang CK, Beraldi E, Jager W, Ettinger S, Fazli L, Nappi L, Bishop J, Zhang F,

Chauchereau A, Loriot Y, Gleave M (2016) Clusterin knockdown sensitizes prostate cancer cells to taxane by modulating mitosis. *EMBO Mol Med* **8**: 761-78

17. Rizzi F and Bettuzzi S (2009) Clusterin (CLU) and prostate cancer. *Adv Cancer Res* **105**: 1-19
18. July LV, Akbari M, Zellweger T, Jones EC, Goldenberg SL, Gleave ME (2002) Clusterin expression is significantly enhanced in prostate cancer cells following androgen withdrawal therapy. *Prostate* **50**: 179-88
19. Rohne P, Prochnow H, Koch-Brandt C (2016) The CLU-files: disentanglement of a mystery. *BioMol Concepts* **7**: 1–15
20. Jo H, Jia Y, Subramanian KK, Hattori H, Luo HR (2008) Cancer cell-derived clusterin modulates the phosphatidylinositol 3'-kinase-Akt pathway through attenuation of insulin-like growth factor 1 during serum deprivation. *Mol Cell Biol* **28:** 4285-99
21. Ammar H and Closset JL (2008) Clusterin activates survival through the phosphatidylinositol 3-kinase/Akt pathway. *J Biol Chem* **283**: 12851-61
22. Ma X and Bai Y (2012) IGF-1 activates the P13K/AKT signaling pathway via upregulation of secretory clusterin. *Mol Med Rep* **6**: 1433-7
23. Manning BD and Toker A. (2017) AKT/PKB Signaling: Navigating the Network. *Cell* **169**: 381-405
24. Ruzzene M, Bertacchini J, Toker A, Marmiroli S (2017) Cross-talk between the CK2 and AKT signaling pathways in cancer. *Adv Biol Regul* **64**:1-8
25. Fruman DA and Rommel C (2014) PI3K and cancer: lessons, challenges and opportunities. *Nat Rev Drug Discov* **13**: 140-56
26. Gao T, Furnari F, Newton AC (2005) PHLPP: a phosphatase that directly dephosphorylates Akt, promotes apoptosis, and suppresses tumor growth. *Mol Cell* **18**: 13-24

27. Newton AC and Trotman LC (2014) Turning off AKT: PHLPP as a drug target. *Annu Rev Pharmacol Toxicol* **54**: 537-58

28. McCubrey JA, Abrams SL, Fitzgerald TL, Cocco L, Martelli AM, Montalto G, Cervello M, Scalisi A, Candido S, Libra M, Steelman LS (2015) Roles of signaling pathways in drug resistance, cancer initiating cells and cancer progression and metastasis. *Adv Biol Regul* **57**: 75-101

29. Bertrand FE, McCubrey JA, Angus CW, Nutter JM, Sigounas G (2014) NOTCH and PTEN in prostate cancer. *Adv Biol Regul* **56**: 51-65

30. Taylor BS, Schultz N, Hieronymus H, Gopalan A, Xiao Y, Carver BS, Arora VK, Kaushik P, Cerami E, Reva B, Antipin Y, Mitsiades N, Landers T, Dolgalev I, Major JE, Wilson, M, Socci ND, Lash AE, Heguy A, Eastham JA, Scher HI, Reuter VE, Scardino PT, Sander C, Sawyers CL, Gerald WL (2010) Integrative genomic profiling of human prostate cancer. *Cancer Cell* **18**: 11-22

31. Chen M, Pratt CP, Zeeman ME, Schultz N, Taylor BS, O'Neill A, Castillo-Martin M, Nowak DG, Naguib A, Grace DM, Murn J, Navin N, Atwal GS, Sander C, Gerald WL, Cordon-Cardo C, Newton AC, Carver BS, Trotman LC (2011) Identification of PHLPP1 as a tumor suppressor reveals the role of feedback activation in PTEN-mutant prostate cancer progression. *Cancer Cell* **20**: 173-86

32. Virtakoivu R, Pellinen T, Rantala JK, Perälä M, Ivaska J (2012) Distinct roles of AKT isoforms in regulating β1-integrin activity, migration, and invasion in prostate cancer. *Mol Biol Cell* **23**: 3357-69

33. Cariaga-Martinez AE, López-Ruiz P, Nombela-Blanco MP, Motiño O, González-Corpas A, Rodriguez-Ubreva J, Lobo MV, Cortés MA, Colás B (2013) Distinct and specific roles of AKT1 and AKT2 in androgen-sensitive and androgen-independent prostate cancer cells. *Cell Signal* **25**: 1586-97

34. Scaltriti M, Bettuzzi S, Sharrard RM, Caporali A, Caccamo AE, Maitland NJ (2004) Clusterin

overexpression in both malignant and nonmalignant prostate epithelial cells induces cell cycle arrest and apoptosis. *Br J Cancer* **91**: 1842-50

35. Chin YR and Toker A (2010) The actin-bundling protein palladin is an Akt1-specific substrate hat regulates breast cancer cell migration. *Mol Cell* **38**: 333-44
36. Maraldi T, Bertacchini J, Benincasa M, Guida M, De Pol A, Liotta LA, Petricoin E, Cocco L, Marmiroli S (2011) Reverse-phase protein microarrays (RPPA) as a diagnostic and therapeutic guide in multidrug resistant leukemia. *Int J Oncol* **38**: 427-35
37. Cenni V, Bertacchini J, Beretti F, Lattanzi G, Bavelloni A, Riccio M, Ruzzene M, Marin O, Arrigoni G, Parnaik V, Wehnert M, Maraldi NM, de Pol A, Cocco L, Marmiroli S (2008) Lamin A Ser404 is a nuclear target of Akt phosphorylation in C2C12 cells. *J Proteome Res* **7**: 4727-35
38. Cenni V, Capanni C, Mattioli E, Columbaro M, Wehnert M, Ortolani M, Fini M, Novelli G, Bertacchini J, Maraldi NM, Marmiroli S, D'Apice MR, Prencipe S, Squarzoni S, Lattanzi G (2014) Rapamycin treatment of Mandibuloacral dysplasia cells rescues localization of chromatin-associated proteins and cell cycle dynamics. *Aging (Albany NY)* **6**: 755-70
39. Maraldi NM, Zini N, Santi S, Bavelloni A, Valmori A, Marmiroli S, Ognibene A (1993) Phosphoinositidase C isozymes in SaOS-2 cells: immunocytochemical detection in nuclear and cytoplasmic compartments. *Biol Cell* **79**: 243-50
40. Bertacchini J, Guida M, Accordi B, Mediani L, Martelli AM, Barozzi P, Petricoin E 3rd, Liotta L, Milani G, Giordan M, Luppi M, Forghieri F, De Pol A, Cocco L, Basso G, Marmiroli S (2014) Feedbacks and adaptive capabilities of the PI3K/Akt/mTOR axis in acute myeloid leukemia revealed by pathway selective inhibition and phosphoproteome analysis. *Leukemia* **28**: 2197-205
41. Serafin V, Lissandron V, Buldini B, Bresolin S, Paganin M, Grillo F, Andriano N, Palmi C, Cazzaniga G, Marmiroli S, Conter V, Basso G, Accordi B (2017) Phosphoproteomic analysis reveals hyperactivation of mTOR/STAT3 and LCK/Calcineurin axes in pediatric early T-cell

precursor ALL. *Leukemia* **31**: 1007-1011

42. Brugnoli F, Grassilli S, Piazzi M, Palomba M, Nika E, Bavelloni A, Capitani S, Bertagnolo V (2013) In triple negative breast tumor cells, PLC-β2 promotes the conversion of CD133high to CD133low phenotype and reduces the CD133-related invasiveness. *Mol Cancer* **12**: 165-180
43. Grassilli S, Brugnoli F, Lattanzio R, Rossi C, Perracchio L, Mottolese M, Marchisio M, Palomba M, Nika E, Natali PG, Piantelli M, Capitani S, Bertagnolo V (2014) High nuclear level of Vav1 is a positive prognostic factor in early invasive breast tumors: a role in modulating genes related to the efficiency of metastatic process. *Oncotarget* **5**: 4320-36
44. Maehama T and Dixon JE (1998) The tumor suppressor, PTEN/MMAC1, dephosphorylates the lipid second messenger, phosphatidylinositol 3,4,5-trisphosphate. *J Biol Chem* **73**: 13375–78
45. Myers MP, Pass I, Batty IH, Van der Kaay J, Stolarov JP, Hemmings BA, Wigler MH, Downes CP, Tonks NK (1998) The lipid phosphatase activity of PTEN is critical for its tumor supressor function. Proc Natl Acad Sci U S A **95**: 13513–8
46. Song MS, Salmena L, Pandolfi PP (2012) The functions and regulation of the PTEN tumour suppressor. *Nat Rev Mol Cell Biol* **13**: 283–96
47. Milella M, Falcone I, Conciatori F, Cesta Incani U, Del Curatolo A, Inzerilli N, Nuzzo C, Ciuffreda L (2015) PTEN: Multiple Functions in Human Malignant Tumors. *Frontiers in Oncology* **5**: 24-38
48. Vazquez F, Ramaswamy S, Nakamura N, Sellers WR (2000) Phosphorylation of the PTEN tail regulates protein stability and function. *Mol Cell Biol* **20**: 5010-8
49. Barata JT (2011) The impact of PTEN regulation by CK2 on PI3K-dependent signaling and leukemia cell survival. *Adv Enzyme Regul* **51**: 37-49
50. Li X, Liu J, Gao T (2009) beta-TrCP-mediated ubiquitination and degradation of PHLPP1 are negatively regulated by Akt. *Mol Cell Biol* **29**: 6192-205
51. Grzechnik AT and Newton AC (2016) PHLPPing through history: a decade in the life of PHLPP

phosphatases. *Biochem Soc Trans* **44**:1675-1682

52. Beezhold K, Liu J, Kan H, Meighan T, Castranova V, Shi X, Chen F (2011) miR-190-mediated downregulation of PHLPP contributes to arsenic-induced Akt activation and carcinogenesis. *Toxicol Sci* **123**: 411-20

53. Wang Q, Cao W, Su Q, Liu Z, Zhang L (2014a) Clusterin silencing inhibits proliferation and reduces invasion in human laryngeal squamous carcinoma cells. *World J Surg Oncol* **12**: 124-131

54. Shi H, Deng JH, Wang Z, Cao KY, Zhou L, Wan H (2013) Knockdown of clusterin inhibits the growth and migration of renal carcinoma cells and leads to differential gene expression. *Mol Med Rep* **8**: 35-40

55. Wang X, Luo L, Dong D, Yu Q, Zhao K (2014b) Clusterin plays an important role in clear renal cell cancer metastasis. *Urol Int* **92**: 95-103

56. Niu Z, Li X, Hu B, Li R, Wang L, Wu L, Wang X (2012) Small interfering RNA targeted to secretory clusterin blocks tumor growth, motility, and invasion in breast cancer. *Acta Biochim Biophys Sin (Shanghai)* **44**: 991-8

57. Wang C, Jiang K, Kang X, Gao D, Sun C, Li Y, Sun L, Zhang S, Liu X, Wu W, Yang P, Guo K, Liu Y (2012) Tumor-derived secretory clusterin induces epithelial-mesenchymal transition and facilitates hepatocellular carcinoma metastasis. *Int J Biochem Cell Biol* **44**: 2308-20

58. Moretti RM, Montagnani Marelli M, Mai S, Cariboni A, Scaltriti M, Bettuzzi S, Limonta P (2007) Clusterin isoforms differentially affect growth and motility of prostate cells: possible implications in prostate tumorigenesis. *Cancer Res* **67**: 10325-33

59. Zhao Z, Robinson RG, Barnett SF, Defeo-Jones D, Jones RE, Hartman GD, Huber HE, Duggan ME, Lindsley CW (2008) Development of potent, allosteric dual Akt1 and Akt2 inhibitors with improved physical properties and cell activity. *Bioorg Med Chem Lett* **18**: 49-53

60. Bulj Z, Duchi S, Bevilacqua A, Gherardi A, Dozza B, Piccinini F, Mariani G, Lucarelli E, Giannini S, Donati D, Marmiroli S (2013) Protein kinase B/AKT isoform 2 drives migration of human mesenchymal stem cells. *Int J Oncol* **42**: 118-26

61. Zhong B, Sallman DA, Gilvary DL, Pernazza D, Sahakian E, Fritz D, Cheng JQ, Trougakos I, Wei S, Djeu JY (2010) Induction of clusterin by AKT-role in cytoprotection against docetaxel in prostate tumor cells. *Mol Cancer Ther* **9**: 1831-41

62. Jin J, Kim JM, Hur YS, Cho WP, Lee KY, Ahn SI, Hong KC, Park IS (2012) Clinical significance of clusterin expression in pancreatic adenocarcinoma. *World J Surg Oncol* **10**: 146-151

63. Shim YJ, Kang BH, Jeon HS, Park IS, Lee KU, Lee IK, Park GH, Lee KM, Schedin P, Min BH (2011) Clusterin induces matrix metalloproteinase-9 expression via ERK1/2 and PI3K/Akt/NF-κB pathways in monocytes/macrophages. *J Leukoc Biol* **90**: 761-9

64. Shim YJ, Kang BH, Choi BK, Park IS, Min BH (2012) Clusterin induces the secretion of TNF-α and the chemotactic migration of macrophages. *Biochem Biophys Res Commun* **422**: 200-5

TITLE AND LEGEND TO FIGURES

Figure 1. **Clusterin enhances the PI3K signaling pathway at multiple levels** (A) Heatmap from the RPPA analysis of PNT1A cells stably transfected with empty vector (MOCK) or with clusterin (CLU). The colors in each cell indicate the signal intensities of single antibodies (RED, high intensity, WHITE low intensity). (B) Bar chart of key components of the PI3K/AKT cascade from (A). X axis reports all endpoints tested (phosphorylated epitopes where indicated); Y axis reports the fold-change ratio of signal intensity in CLU versus MOCK samples. The arbitrary unit of MOCK was set as 1, while the cutoff magnitude to qualify changes in specific proteins phosphorylation as significant was set as 1.2-fold. (C) Lysates from the above analysis were resolved by Western blot and probed with the indicated antibodies. Note that the anti-AKT S473 antibody detects both phosphorylated AKT1 S473 and AKT2 S474. The lower panel shows comparison of AKT1 and 2 isoforms, both total and phosphorylated, in MOCK and CLU lysates by means of isoform-specific antibodies. The lower right panel shows AKT2 and AKT1 silencing in CLU cells by isoform-specific shRNA. CLU cells transfected with scramble shRNA were run as control. (D) Bar panel with quantitation of signal intensity of each band, normalized to the loading control, as optical densities (OD) ratio of phosphorylated *versus* total protein. (E) PIP3, PIP2 and CLU immunfluorescence analysis. Representative immunofluorescence photomicrographs of MOCK and CLU cells, showing PIP3, PIP2 and CLU content. Dilution: anti-PIP3 and anti-PIP2 (Echelon Laboratories), 1:50 dilution; anti-CLU, 1:100 (Millipore). Images were taken at a magnification of 60X.

Figure 2. Analysis of PHLPP1 levels in CLU overexpressing cells. PHLPP1 was analyzed by Western blot in protein extracts from MOCK and CLU cells, and from PNT1A cells transfected with empty vector (ev) or with CLU (CLU) for 24 hours, as indicated, then probed with anti-PHLPP1 from Bethyl Laboratories, 1:1000. Lower panel, actin loading control.

Figure 3. **Modulation of PHLPP1 expression by CLU**. (A) RT-PCR analysis of PHLPP1 mRNA in PNT1A and PC3 cells. CLU was either overexpressed (CLU) or silenced with specific siRNA (siRNA) by transfection for 72 hours. Control cells were transfected with empty vector (ev) or with a scrambled sequence (scramble). (B) miR-190 levels were determined by RT-PCR in MOCK, CLU and PNT1A cells from (A). (C) CLU expression was probed in all the above experimental points by anti-clusterin Western blot followed by anti-actin control of protein loading. Results represent the means from three independent experiments ± s.d.

Figure 4. **CLU stimulates migration of normal prostate cells**. (A) Bar graph representation of cell migration analysis by transwell assay. Aliquots of the cells from the experimental points described in Fig. 3A-B were seeded on transwells to analyze cell migration. Relative migration was quantified by counting the number of violet and blue cells (HEMA staining) in three inserts. At least three different experiments were performed. Results are average ± s.d. Silencing of CLU in CLU cells by transfection with specific siRNA for 72 hours (which were not included in the experimental set above) was confirmed by Western blot (figure A insert). Control CLU cells were transfected with a scramble sequence. (B) To verify whether modulation of CLU expression affects cell proliferation or cell viability, aliquots of cells from the above experimental points were analyzed for cell cycle progression by PI staining followed by flow cytometry (left panels) and for cell proliferation by MTT assay (right panels).

Figure 5. Effect of AKT isoform-silencing on CLU-stimulated cell migration. (A) Bar graph shows relative migration of MOCK and CLU cells following AKT1 or AKT2 silencing with isoform-specific shRNAs. Migration was quantified by HEMA staining in three inserts, as described above. (B) Samples from each experimental point were resolved by Western blot and probed with isoform-specific antibodies to confirm silencing. (C) Relative migration of MOCK and CLU cells 48 hours upon addition to the growth medium of the specific AKT2 inhibitor (XII)

at 0.5 μM. Relative migration was quantified as described above. (D) AKT2 inhibition was confirmed by Western blotting with anti-pAKT1/2. At least three different migration experiments were performed. Results are average ± s.d.

Figure 6. Modulation of normal and cancer cell motility by CLU. PNT1A and PC3 cells from the same pool analyzed in Figure 3 (transfected with empty vector or with CLU) were run with the xCELLigence System to evaluate modulation of migration (A) and invasion (B) by CLU. The relative migration index is indicated in Y axis. Migration and invasion experiments were repeated two times. Results are average ± s.d.

Supplemental Information

Title and Legend to Supplementary Figures and Tables.

Figure 1S. Analysis of key signaling pathways in CLU *versus* MOCK cells. (A-F) Bar chart representation of key signaling pathways. X axis, endpoints tested (phosphorylated epitopes where indicated); Y axis, fold-change ratio of signal intensity of CLU *versus* MOCK samples. The arbitrary unit of MOCK was set as 1.

Figure 2S. **Effect of Okadaic acid on AKT T308 phoshorylation**. To indirectly evaluate PP2A activity, MOCK and CLU cells were treated with 500 nM Okadaic acid for 1 hour. Akt T308 phosphorylation was monitored by Western blot. Actin control loading is shown. Optical density of pT308 normalized to actin loading controls is reported in the table as well as in the lower panel.

Figure 3S. **RPPA analysis of GSK3 Y216/Y279 and β-catenin S33/S37/T41 epitopes**. A bar plot is shown, where Y represents the fold change calculated by measuring ratios of signal intensity in CLU *versus* MOCK samples. The arbitrary unit of MOCK was set as 1.

Legend to Table 1. **Antibodies list**. A complete list of the antibodies used in this work, their source and dilution are shown.

Legend to Diagram 1S. CLU modulates motility of prostate cells PHLPP1 down-modulation through and AKT2 activation. Schematic diagram showing the mechanistic explanation of how CLU overexpression could lead to increased cell motility. Our results indicate that sCLU activates AKT signaling acting at several levels of the PI3K pathway. In particular, hyperactivation of AKT2 is due to down-modulation of the specific AKT2 S474 phosphatase, PHLPP1, by increased miR-190 levels. Phosphorylated AKT2, in turn, boosts migration of normal human prostate cells exposed to sCLU, and invasion of the human highly tumorigenic PC3 cells.